Hindawi
Advances in Civil Engineering
Volume 2018, Article ID 6415763, 8 pages
https://doi.org/10.1155/2018/6415763

Research Article

Identification of Hydrochemical Function and Behavior of the Houzhai Karst Basin, Guizhou Province, Southwestern China

Xian Li and Yanqiao Wang

School of Civil Engineering, Hefei University of Technology, Hefei 230009, China

Correspondence should be addressed to Yanqiao Wang; wangyq0726@163.com

Received 17 December 2017; Accepted 9 January 2018; Published 13 March 2018

Academic Editor: Hang Lin

Due to the difference of geomorphology and the development of fractures, the hydrochemical function and behavior appear to be complex. Variations of karst water conductivity can reflect the contribution of different runoff sources and thus indirectly reflect the development characteristics of conduits and fractures. Taking Houzhai karst system (southwestern China) as a case study, the frequency distribution curves of karst water conductivity were decomposed by Gaussian Mixture Analysis to identify the runoff components of different karst landform. The dominant runoff types had been distinguished, and the relative contribution of the different water types had been investigated. The results showed that the karst flow types were slope flow, rapid fracture flow, and slow fracture flow. Rapid fracture flow was the major recharge type of Houzhai karst water system. Slow fracture flow in the downstream area accounted for a larger proportion than that of the upstream area. The relative contribution of the different runoff components showed that the upstream area was a rapid flow area of conduit structure with low storage capacity, the downstream area was an aquifer spatial structure of netted fissure conduit with high storage capacity, and the midstream area was a transitional zone between the upstream and downstream area.

1. Introduction

Hydrochemical responses can rapidly reflect the heterogeneous karst water system for the rainfall input signal events [1, 2]. The most significant influence of rainfall on the chemical dynamics of karst water is the dilution effect. That is, with the increase of precipitation, especially in heavy rainfall, karst water can be recharged by adequate precipitation. Due to the large amount conduit of karst water system, making the rapid infiltration rate of precipitation, the chemical concentrations of karst water reduce rapidly. The response characteristics of chemical dynamic of karst water to precipitation reflect the characteristics of groundwater recharge process, runoff, landform type, and fracture development in the karst aquifer system [3–5]. In the same karst basin, for different landform combination types with different carbonate rock outcrop conditions and different development degrees of karstification, even under the same rainfall intensity, karst water chemical dynamic response of different landform combinations to precipitation is not the same. Hydrochemical responses in a karst conduit system are more sensitive than those in a porous and narrow fissured karst system [6].

Conductivity refers to the ability of the solution to conduct electricity and reflects the amount of total dissolved solids (TDS) in the water, whereas karst water is dominated by the balance of calcium carbonate. Variations of karst water conductivity can reflect the contribution of different runoff sources to the karst water system, which can be either exogenous water that reaches the karst water system through the sinkhole, disperse permeate recharge water, or store in small fractures base flow [7]. These can also indirectly reflect the development characteristics of conduits and fractures. Shuster and White [8] proposed in 1971 that the coefficient of variation of conductivity of karst water can be used to classify the hydrodynamic characteristics of karst water systems; the karst water system with variation coefficient less than 5% is dominated by dispersed flow, whereas the karst aquifer system with variation coefficient more than 5% is dominated by conduit flow. Newson [9] and Worthington et al. [10]

pointed out that the coefficient of variation of hardness or conductivity of karst water can be used as an indicator of the source division of runoff components of karst aquifer system. Bakalowicz and Manign [11] showed that the karst water conductivity distribution can provide more accurate information about karst aquifer system based on the studies of several karst aquifers in France. Some conductivity frequency distributions of karst water system were unimodal distribution, while some were multimodal distribution, with a very wide concentration range. Therefore, it is not enough to describe the hydrodynamic characteristics of karst system by using the statistical parameter of variation coefficient alone. The conductivity frequency distribution curve of karst water reflects the karst water mineralization and chemical composition of the dynamic variability. Carbonate distribution basically controls the hydrochemical characteristics, hydrochemical type, and spatial hydrochemical distribution of karst water. Precipitation also plays an important role in the formation of hydrochemical features. Under the combined influence of precipitation dilution, geology of underlying surface, and karst geomorphology, different hydrogeological units have different characteristics of subsurface flow processes. In the karst aquifer system, the frequency distribution curve of water chemical variables showed a multipeak distribution, with different peaks representing different water sources and occupying the corresponding proportions.

In this paper, the research focuses on the decomposition of the frequency distribution curve of karst water conductivity by Gaussian mixture analysis and expectation-maximization algorithm to divide runoff components of different karst landform combination types. The results can give an insight on the hydrodynamic behavior and the fracture development degree of karst system.

2. Study Area

Guizhou Houzhai karst basin (Figure 1) is located in the south of Puding County, Guizhou Province, southwestern China, with an area of 81 km^2. The basin in the southeast is higher than that in the northwest where the altitude is between 1220 and 1400 m above sea level. The carbonate rocks in the basin are widely distributed. The main aquifers of the basin are comprised of limestone and dolomite of the Middle Triassic Guanling formation (T_2g). The Middle Triassic Guanling Formation can be divided into three members including T_2g^1, T_2g^2, and T_2g^3 (Figure 2). The first member of the Guanling Formation (T_2g^1) occurs mainly in the upstream of the basin. The second member (T_2g^2) occurs in the area from Chenqi, Maguanto Sanjianfang. The third member (T_2g^3) occurs in the area from Pingshan to Maoshuikeng [3]. There are several surface rivers and underground rivers developed in the basin, which generally flow from east to west.

There are three kinds of landform combination types (Figure 1) which control different forms of water recharge and transformation process. The first landform combination type is the peak-cluster depression which mainly occurs in the upstream area, northeast of Houzhai karst basin. The area is almost exposed karst area and no surface river. The land surface exhibits closed depressions which often contain funnels, sinkholes, or vertical shafts. Overland runoff resulting from large storms flows into the underground river systems faster along the funnels, sinkholes, or vertical shafts. The infiltration process mainly occurs in the fractures and conduits, where the hydraulic gradient is larger. The depth to groundwater is mostly greater than 15 m. The second landform combination type is the peak-cluster valley and trough valley combination type distributed in the midstream area which is a transition zone from peak-cluster depression to peak-cluster basin. Surface rivers and underground rivers alternate with each other. The area is covered by thin layer soil. The depth to groundwater is shallow, ranging from 1 to 10 m. Moreover, the groundwater flow is mainly horizontal. The third landform combination type is a peak-cluster basin, and hilly combination type occurs in the downstream area. The area is covered by thick layer soil. The downstream zone is characterized by an aquifer spatial structure of netted fissure conduit with high storing and regulation power. The depth to groundwater is shallow, and the underground river has formed a large exit at Maoshuikeng [12].

3. Methods

3.1. Gaussian Mixture Analysis (GM). Gaussian mixture analysis [13], also known as frequency distribution analysis method, is a statistical clustering algorithm. The frequency distribution curve can be decomposed into multiple Gaussian distribution curves; each of the different Gaussian distribution curves represents different components which occupy the corresponding relative proportion. In this paper, the conductivity frequency distribution curve of karst water is decomposed to several Gaussian distribution curves. Each Gaussian distribution curve obtained by decomposition represents the frequency distribution of a runoff component. The probability density function of data $X(t)(x \in R^d)$ is assumed to be $p(x)$, which is a mixture of H Gaussian components. The model can be expressed as follows:

$$P(x|\lambda) = \sum_{i=1}^{H} k_i f_i(X), \tag{1}$$

where $\sum_j k_i = 1$, $i = 1, 2, \ldots, H$; k_i are mixed weighting coefficients; and $f_i(X)$ obeys the Gaussian distribution with expectation u_i and variance σ_i^2.

So, the Gaussian mixture probability density function can be characterized by the expected u_i, the variance σ_i^2, and the mixing weighting factors of the Gaussian probability density of all components:

$$\lambda_i = \{u_i, \sigma_i, k_i\}, \quad u_1 < u_2 < \cdots < u_H. \tag{2}$$

Then, these unknown parameters ($k_1, \ldots, k_H$; $u_1, \ldots, u_H$; $\sigma_1, \ldots, \sigma_H$) should be calculated. Suppose there is a density function controlled by the parameter vector λ, where the function $L(\lambda|X)$ is called the likelihood function and is the parameter λ function parameter determined by the observation vector X:

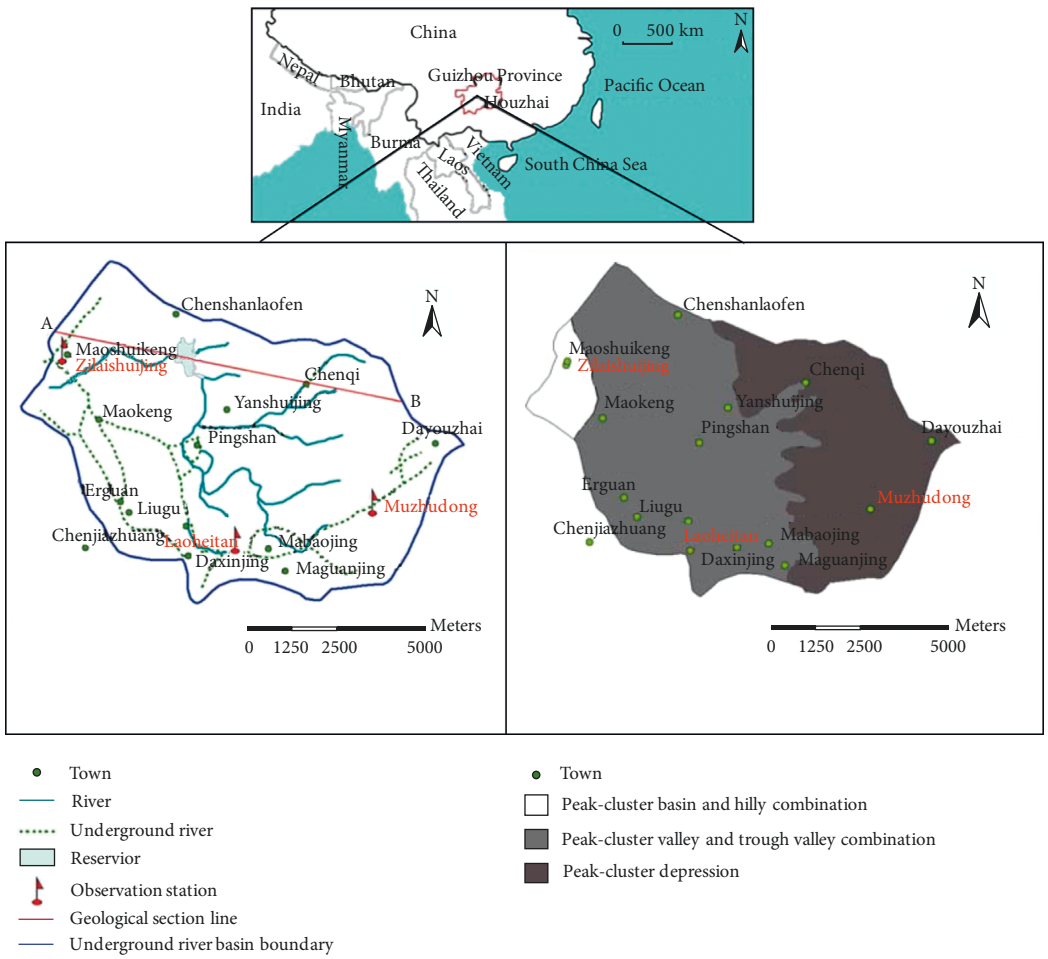

Figure 1: The location map and the landform types map of Houzhai karst basin in Guizhou Province, China [3].

$$P(x|\lambda) = \sum_{i=1}^{H} k_i f_i(X) = L(\lambda|X),$$
$$\lambda^* = \arg\max_{\lambda} L(\lambda|X). \tag{3}$$

These unknown parameters can be calculated by the expectation-maximization algorithm presented in the following section. The goal of maximization is to find the parameter λ^*.

3.2. Expectation-Maximization Algorithm (EM). The expectation-maximization Algorithm (EM) [14] is an algorithm that looks for the parameter maximum likelihood or maximum a posteriori estimates in a probabilistic model where the probabilistic model relies on unobservable implicit variables, that is, the maximum likelihood estimation of distribution parameters can be calculated from incomplete data.

Suppose that data X is incomplete data which is observed and constructed according to a certain distribution. Suppose that the complete data set $Z = (X, Y)$ is formed after the missing data Y is introduced. The joint density function of Z is

$$p(z|\theta) = p(x, y|\theta) = p(y|x, \theta)p(x|\theta). \tag{4}$$

The joint density function is mainly calculated from the edge density function and hidden variables. Define a new likelihood function:

$$L(\theta|z) = L(\theta|X, Y) = p(X, Y|\theta) = h_{x,\theta}(Y). \tag{5}$$

The EM algorithm estimates the unknown data Y from the known observed data and the current parameter, so the expected value of the complete data of the likelihood function $p(X, Y|\theta)$ can be estimated:

$$Q\left(\theta, \theta^{(i-1)}\right) = E\left[\ln p(X, Y|\theta)\middle|X, \theta^{(i-1)}\right]$$
$$= \int_{y\in\gamma} \ln p(X, y|\theta) f\left(y\middle|X, \theta^{(i-1)}\right) dy. \tag{6}$$

$\theta^{(i-1)}$ is the current parameter used to estimate the expected value, and θ is the new parameter after iteration. θ is a formal variable that can be adjusted, and Y is a random variable controlled by the function $f(y|X, \theta^{(i-1)})$. $f(y|X, \theta^{(i-1)})$ is the edge density function of unobserved data, which is determined by the observation data X and the parameters θ. γ is the value range of y. For the

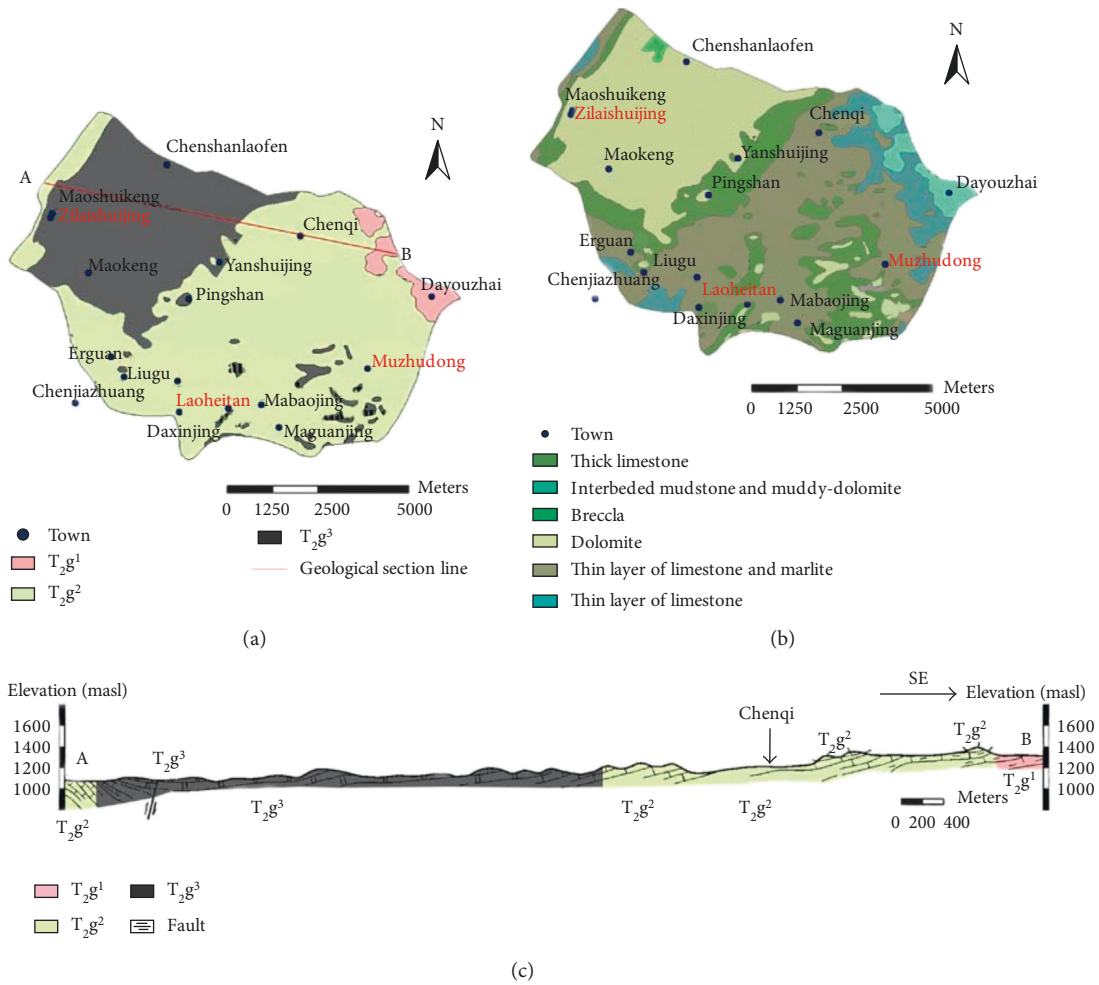

Figure 2: The formation and lithology of the Houzhai karst basin. (a) Members of the Guanling Formation. (b) Lithology. (c) Simplified geological cross-section AB [3].

function $h(\theta, Y)$, there is a deterministic function that can be maximized:

$$E_Y[h(\theta, Y)] = \int_y h(\theta, Y) f_Y(y) dy. \quad (7)$$

4. Data Characteristics and Analysis

According to the runoff and transformation process of karst water in Houzhai karst basin, the water sources of the karst water runoff in Houzhai karst basin were divided into three types, including slope flow, rapid fractured flow, and slow fractured flow (Figure 3). Different water sources have different boundary conditions and different flow concentration rates. Slope flow recharged from excess infiltration reaches the outlet fast through the underground rivers, and its discharge hydrograph rises and declines rapidly. Rapid fracture flow reaches the outlet through large fissure network and underground rivers after being transferred to storage. The concentration velocity is slower than that of slope flow, and the degree of regulation and storage is larger than that of slope flow. The slow fracture flow reaches the outlet section through narrow fissures network and underground rivers. The concentration velocity is less than that of the fast fracture flow, and the degree of regulation and storage is greater than that of the rapid fracture flow [15].

In this paper, the conductivity time series data of three representative monitoring stations (Muzhudong, Laoheitan, and Zilaishuijing) in the upperstream, middlestream, and downstream area, respectively, from 1990 to 1992 were analyzed. The monitoring data were managed and maintained by the staff in the local karst study institution.

According to the discharge hydrograph of three stations in 1991 (Figure 4), it can be seen that the spring hydrograph of the upstream Muzhudong station displays a spike type with large discharge variation and short lag time to precipitation. The spring hydrograph of the downstream Zilaishuijing station showed a smooth type with a longer lag time to precipitation. The spring hydrograph of the middlestream Laoheitan station was smoother than that in upstream but sharper than that in downstream, and flood peak flow is less than the Muzhudong station.

Therefore, different hydrological and geomorphological structural units have different water flow characteristics including recharge mode, water transformation process, and runoff regulation, and these differences also lead to the difference in the chemical characteristics of karst water.

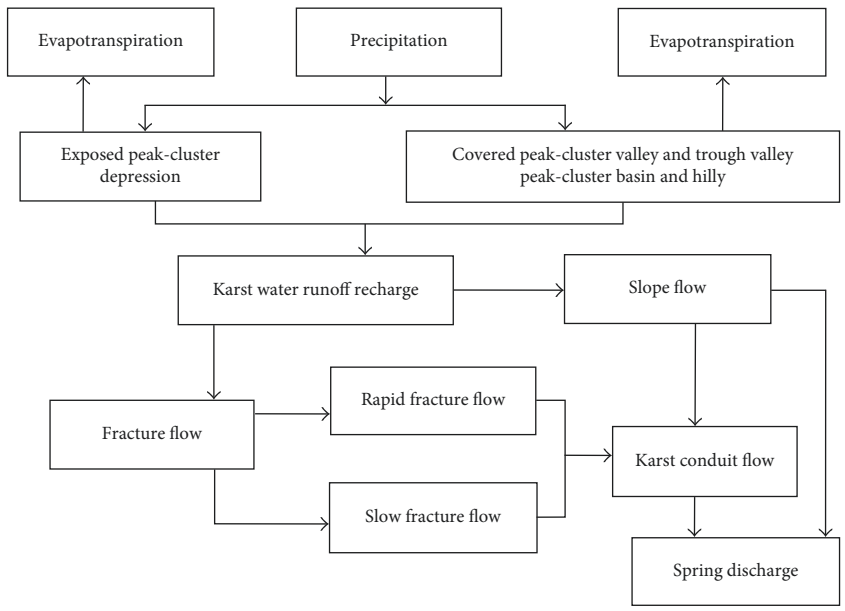

Figure 3: The karst runoff process of Houzhai kasrt basin.

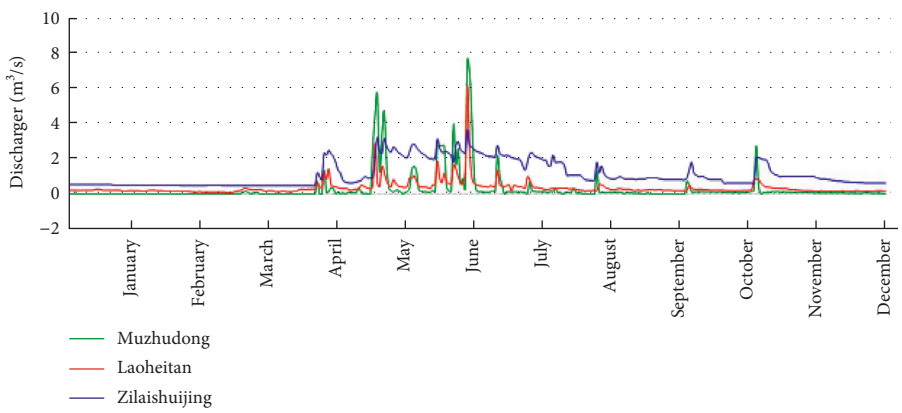

Figure 4: Discharge hydrograph of Houzhai karst water in 1991.

5. Results and Discussion

By using the Gaussian mixture analysis method and the expectation-maximization algorithm, the conductivity frequency distribution curves of three representative stations (Muzhudong, Laoheitan, and Zilaishuijing)in three water years were decomposed respectively (Figure 5). From Figure 5, there were four different runoff components (P_1, P_2, P_3, and P_4), where P_1 was in the lower conductivity distribution, P_4 was in the higher conductivity distribution, and P_2 and P_3 were in the middle of the conductivity distribution.

Judging from the conductivity distribution range, it is assumed that P_1 represents slope flow. When the rainfall intensity exceeds the infiltration capability of the fracture, the excess-infiltration precipitation form slope flow converges to the funnels and the sinkholes and recharges the underground river in a concentrated way. The discharge of P_1 runoff was large, and its rate was fast with short residence time. Their conductivity value was in the lower distribution range because the runoff was easy to dilute with lower chemical ion concentration. P_4 represents slow fracture flow which penetrated along smaller fissures, moved slowly in the rock mass and secondary fissures, and formed the basic flow of the underground river. The recharge time is long, and the discharge was small. The chemical concentration of slow fracture flow was high and in the higher distribution range. P_2 and P_3 represent rapid fracture flow. Their chemical concentration values were between the values of the slope flow and the slow fracture flow. After precipitation infiltrated downward from the surface and encountered larger fissures or fractures, rapid fracture flow was formed to directly recharge the underground conduit.

Due to different fracture sizes, rapid fracture flows were formed with different convergence velocities. P_2 and P_3 were likely to be two different rapid fracture flows. The conductivity of P_3 is greater than P_2, suggesting that the

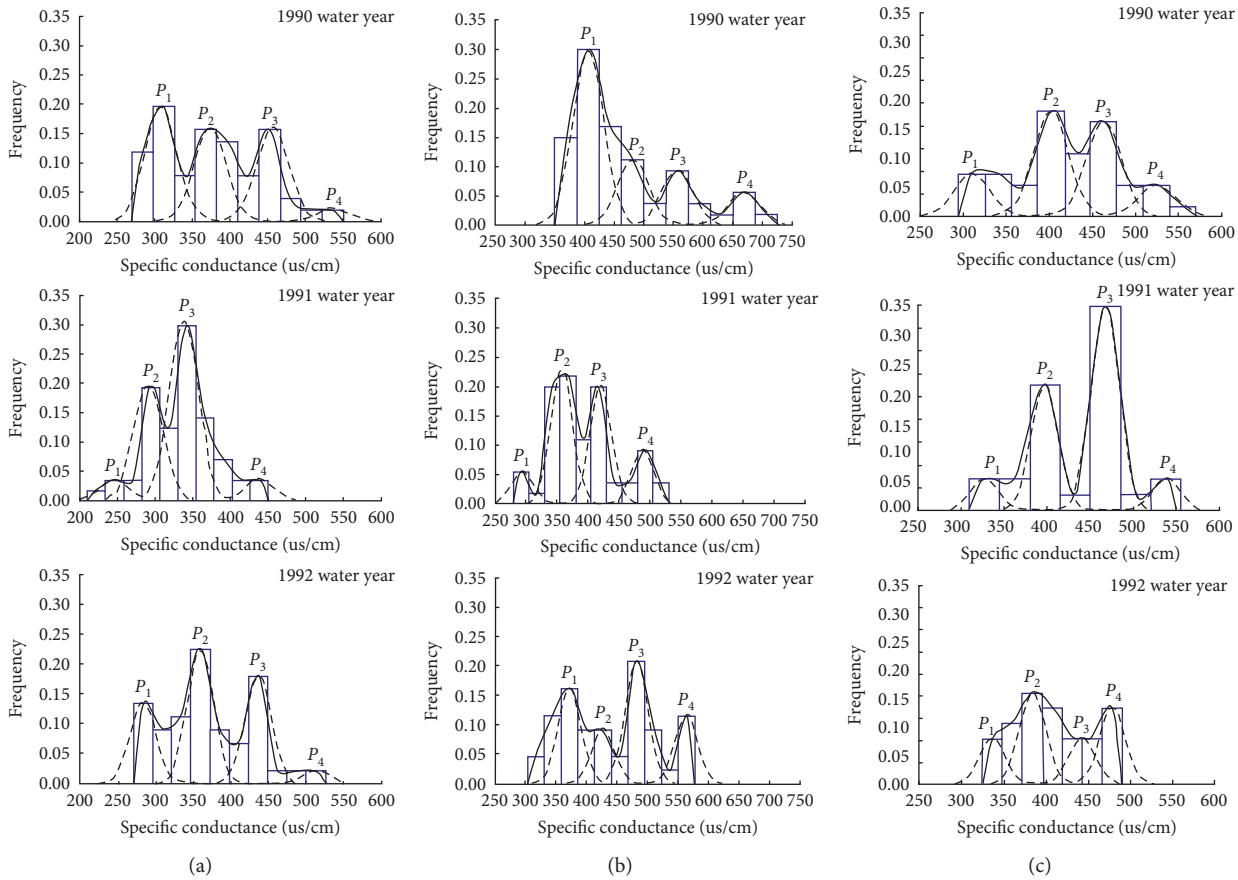

Figure 5: Specific frequency distribution curves of three stations in different water year. (a) Muzhudong station. (b) Laoheitan station. (c) Zilaishuijing station.

Table 1: The relative contribution of the different runoff components of three stations.

Station	Water year	P_1 (%)	P_2 (%)	P_3 (%)	P_4 (%)	Discharge (m^3/s)	Precipitation (mm)
Muzhudong	1990	36.75	29.6	29.78	3.88	0.119	1093.7
	1991	6.28	34.25	53.19	6.28	0.316	1806
	1992	24	40	32	4	0.168	1271.8
	Average	22.34	73		4.72	0.201	1390.5
Laohetan	1990	53.33	20	16.67	10	0.244	1129.6
	1991	7.83	40.26	35.77	16.14	0.43	1726.9
	1992	28	16	36	20	0.312	1320.7
	Average	29.72	54.9		15.38	0.329	1392.4
Zilaishujing	1990	15.38	38.46	34.62	11.54	0.758	1184.5
	1991	8	32	52	8	0.918	2404.7
	1992	17.65	35.29	17.65	29.41	0.839	1390.9
	Average	13.68	70		16.32	0.838	1660
Average		21.9	66.0		12.1	0.456	1481

concentration rate of P_3 may be slower than that of P_2. Table 1 shows the relative contributions of different runoff components at three stations from 1990 to 1992, respectively.

From Figure 5 and Table 1, we can conclude the following:

(1) The relative contributions of P_2 and P_3 at the three stations were the largest than those of P_1 and P_4, indicating that the underground runoff in Houzhai karst basin was dominated by rapid fracture flow with an average contribution degree of 66%. The average contribution of slope flow (P_1) was 21.9% and that of slow fracture flow (P_4) is 12.1%. Thus, it can be seen that Houzhai karst basin is a well-developed karstified system.

(2) Slow fracture flow (P_4) in the downstream Zilaishuijing station accounts for the largest proportion (16.32%) than the upstream and middlestream which account for only 4.72% and 15.38%, respectively. It can be seen that the storage capacity of karst aquifer system in the Houzhai karst basin increases gradually from the upstream to the downstream. The downstream area was covered by a thick layer of lateritic sediments, which can slow the rapid infiltration of rainfall. The karst horizontal morphology is more developed than that of the vertical morphology. The groundwater movement was dominated by horizontal movement.

(3) From the two graphs in Figures 5(a) and 5(b), it showed a leftward shift of the distribution range of conductivity of karst water in 1991 (relative wet year) on the coordinate axis, indicating that, in the wet year, conductivity of karst water and the distribution range of conductivity became smaller as precipitation increased. However, from the graph in Figure 5(c), the distribution range of conductivity did not change with the variation of precipitation. It also showed that the chemical dynamics of groundwater in the downstream was relatively stable, and the storage capacity of groundwater in downstream area is greater than that of the upstream and middlestream area.

(4) The contribution degree of slope flow was relatively larger at upstream Muzhudong Station and middlestream Laoheitan Station accounting for 22.34% and 29.72%, respectively, while the contribution degree of slope flow in the downstream Zilaishuijing station was only 13.68%. The karst vertical morphology of upstream and middlestream area were more developed than that of downstream. Vertical sinkholes and funnel at upstream and middlestream areas in Houzhai karst basin are widely distributed, and they often connect to these underground river systems. Overland runoff resulting from large storms flows into the underground river systems faster along the funnels, sinkholes, or vertical shafts.

6. Conclusions

The results of this research obtained through the decomposition of the frequency distribution curve of karst water conductivity suggest that the karst water sources in Houzhai karst basin are composed of three runoff components, including slope flow, rapid fracture flow, and slow fracture flow.

The relative proportions of different runoff components can reflect the different storage capacities of different karst landform types and development degrees of fractures. The rapid fracture flow accounts for the largest proportion of karst water in the whole karst basin. The slow fracture flow accounts for a relatively larger proportion in the downstream, and the proportion of slope flow in the upstream Muzhudong station and middlestream Laoheitan station is relatively larger.

The storage capacity of downstream area is significantly higher than that of the upstream and middlestream areas. The runoff of karst water recharged by the precipitation is in different ways. The spatial distribution of this runoff is directly controlled by the distribution of karst groundwater systems and its dynamic processes. Concentrated recharge and diversion of leakage recharge are the main recharge ways of runoff in bare karst areas while the concentrated recharge and dispersive infiltration recharge are the main recharge modes in the covered karst regions. The frequency distribution curve of karst aquifer conductivity can well reflect the hydrological characteristics of karst water and the composition of runoff components. And this method can indirectly reflect the development degree of karst fractures and karst landform types.

Conflicts of Interest

The authors declare that they have no conflicts of interest regarding the publication of this paper.

References

[1] T. C Atkinson, "Diffuse flow and conduit flow in limestone terrain in the Mendip Hills, Smoerset (Great Britain)," *Journal of Hydrology*, vol. 35, no. 1-2, pp. 93–103, 1997.

[2] L. Eisenlohr, L. Kiraly, M. Bouzelboudjen, and Y. Rossier, "Numerical simulation as a tool for checking the interpretation of karst spring hydrographs," *Journal of Hydrology*, vol. 193, no. 1–4, pp. 306–315, 1997.

[3] L. H. Liu, L. C. Shu, X. H. Chen, and T. Oromo, "The hydrologic function and behavior of the Houzhai underground river basin, Guizhou Province, southwestern China," *Hydrogeology Journal*, vol. 18, no. 2, pp. 509–518, 2010.

[4] Y. L. Zhao, S. L. Luo, Y. X. Wang, L. Zhang, and W. Wan, "Numerical analysis of Karst water inrush and a criterion for establishing the width of water-resistant rock pillars," *Mine Water and the Environment*, vol. 36, no. 4, pp. 508–519, 2017.

[5] Y. L. Zhao, J. Z. Tang, Y. Chen et al., "Hydromechanical coupling tests for mechanical and permeability characteristics of fractured limestone in complete stress–strain process," *Environmental Earth Sciences*, vol. 76, no. 1, pp. 1–18, 2016.

[6] M. Mudarra and B. Andreo, "Relative importance of the saturated and the unsaturated zones in the saturated and the unsaturated zones in the hydrogeological functioning of karst aquifers: the case of Alta Cadena (Southern Spain)," *Journal of Hydrology*, vol. 397, no. 3-4, pp. 263–280, 2011.

[7] W. B. White, "Conceptual models for karst aquifers," *Speleogenesis and Evolution of Karst Auifers*, vol. 1, no. 1, pp. 1–6, 2003.

[8] E. T. Shuster and W. B. White, "Seasonal fluctuations in the chemistry of limestone springs: a possible means for characterizing karst aquifers," *Journal of Hydrology*, vol. 14, no. 2, pp. 93–128, 1971.

[9] M. D. Newson, "A model of subterranean limestone erosion in the British Isles based on hydrology," *Transactions of the Institute of British Geographers*, vol. 54, pp. 55–70, 1971.

[10] S. R. H. Worthington, G. J. Davies, and J. F. Quinlan, "Geochemistry of spring in temperate carbonate aquifers: recharge type explains most of the variation," in *Procedings of*

Colloque d'Hydrologie en Pays Calcaire et en Milieu Fissure´ (5th Neuchâtel, Switzerland), vol. 11, pp. 341–347, Annales Scientifique de l'Universite´ de Bescancxon, Geologie–Me ´moires Hors Se´rie, Neuchâtel, Switzerland, November 1992.

[11] M. Bakalowicz and A. Mangin, "L'aquifére karstique. Sa définition, ses caractéristiques et son identification," *Mém Horssérie Soc Géol Fr*, vol. 11, pp. 71–79, 1980.

[12] H. Y. Chen and B. Y. Chen, "Lithologic characteristics of Houzhai karst small valley, Puding Guizhou province," *Guizhou Geology*, vol. 22, no. 4, pp. 284–288, 2005, in Chinese.

[13] R. Winson, "Multiresolution gaussian mixture models: theory and application," Department of Computer Science Research Report, Department of Computer Science, University of Waiwick, Coventry, UK, 1999.

[14] J. A. Bilmes, "A gentle tutorial of the EM algorithm and its application to parameter estimation for gaussian mixture and hidden markov models," Tech. Rep. ICSI-R-02, International Computer Science Institute, Berkeley, CA, USA, 1998.

[15] J. B. Yu, L. Z. Yang, and M. Z. Fang, *Typical Study on Developmental Regularity of Karst in China—Assessment and Utilization of Water Resources in the Southern Puding, Guizhou Province*, Publishing House of Science, Beijing, China, 1990, in Chinese.